

# Characterization of thermal transport in one-dimensional microstructures using Johnson noise electro-thermal technique

Jing Liu · Xinwei Wang

Received: 18 September 2014 / Accepted: 10 February 2015 / Published online: 20 February 2015  
© Springer-Verlag Berlin Heidelberg 2015

**Abstract** This work reports on the development of a Johnson noise electro-thermal (JET) technique to directly characterize the thermal conductivity of one-dimensional micro-/nanoscale materials. In this technique, the to-be-measured micro-/nanoscale sample is connected between two electrodes and is subjected to steady-state Joule heating. The average temperature rise of the sample is evaluated by simultaneously measuring the Johnson noise over it and its electrical resistance. The system's Johnson noise measurement accuracy is evaluated by measuring the Boltzmann constant ( $k_B$ ). Our measured  $k_B$  value ( $1.375 \times 10^{-23}$  J/K) agrees very well with the reference value of  $1.381 \times 10^{-23}$  J/K. The temperature measurement accuracy based on Johnson noise is studied against the resistance temperature detector method, and sound agreement (4 %) is obtained. The thermal conductivity of a glass fiber with a diameter of  $8.82 \mu\text{m}$  is measured using the JET technique. The measured value  $1.20 \text{ W/m K}$  agrees well with the result using a standard technique in our laboratory. The JET technique provides a very compelling way to characterize the thermophysical properties of micro-/nanoscale materials without calibrating the sample's resistance–temperature coefficient, thereby eliminating the effect of resistance drift/change during measurement and calibration. Since JET technique does not require resistance–temperature correlation, it is also

applicable to semi-conductive materials which usually have a nonlinear  $I$ – $V$  relation.

## 1 Introduction

Researchers are showing keen interest in one-dimensional micro-/nanoscale materials for their special mechanical, thermal, electrical characteristics and applications in microelectro-mechanical systems (MEMS) and nanoelectro-mechanical systems (NEMS). To investigate the thermo-physical properties of individual one-dimensional micro-/nanostructures, intensive work has been devoted to properties characterization. To date, the  $3\omega$  method [1, 2], the microfabricated device method [3–5], the optical heating electrical thermal sensing (OHETS) technique [6] and the pulsed laser-assisted thermal relaxation (PLTR) [7] technique have been developed. For the  $3\omega$  method, it detects the  $3\omega$  signal in the specimen during self-Joule heating to study the resistance change, which is used to determine thermal diffusivity and thermal conductivity. This technique works when the sample has a linear  $I$ – $V$  behavior within the applied voltage range [1, 2]. However, a large number of microwires/microtubes exhibit semi-conductive properties. The microfabricated device method makes the one-dimensional sample as the thermal path between two suspended islands that are thermally isolated to each other. The thermal conductance of the connecting sample can be determined from the relationship between the temperature rise of both islands and the Joule power applied to one of the island [3–5]. For the OHETS technique, a periodically modulated laser beam irradiates the sample to induce a periodical temperature change and thus leads to a periodic resistance change of the sample. Meanwhile, a small DC current is fed through the sample

---

J. Liu · X. Wang (✉)  
Department of Mechanical Engineering, 2010 Black Engineering  
Building, Iowa State University, Ames, IA 50011, USA  
e-mail: xwang3@iastate.edu

X. Wang  
School of Environmental and Municipal Engineering, Qingdao  
Technological University, Qingdao 266033, Shandong,  
People's Republic of China

to probe its periodical temperature variation due to the periodical resistance change. Thermal properties of the sample can be determined by fitting the phase shift between the voltage variation and the modulated laser beam [6]. This technique can be used to measure the thermophysical properties of conductive, non-conductive and semi-conductive one-dimensional micro-/nanoscale structures. It takes a relatively long measurement time (several hours) for both the OHETS technique and the  $3\omega$  method.

Another technique entitled transient electro-thermal technique (TET) [8, 9] is also developed to characterize the thermophysical properties of micro-/nanoscale materials. In the TET technique, a to-be-measured fiber (the fiber will be coated with a metallic film if it is non-conductive) is suspended between two copper electrodes. At the beginning of the experiment, a DC current is fed through the fiber to induce Joule heating. The temperature change caused by the Joule heating of the fiber will lead to its resistance change, which will cause a change of the voltage over the fiber. The voltage evolution of the sample will be monitored by an oscilloscope and a relative temperature evolution is also derived with the known voltage variation. Once the temperature evolution is obtained, the thermal diffusivity of the fiber can be obtained by fitting the temperature change curve against time. Furthermore, a temperature–resistance calibration procedure has to be taken to determine the temperature coefficient of resistance ( $R$ ) for the samples. Finally, the thermal conductivity of the sample can be determined.

Even though the TET technique has been used well and widely for measuring various samples, some disadvantages do really exist and limit the application of the TET technique to some particular materials. First, the resistance of some materials can be affected by many factors, like stress and strain. So during the  $R$ – $T$  calibration, if the sample is relaxed or stretched, the strain and stress effect cannot be precisely captured, so the real temperature–resistance relation could not be obtained precisely. Second, for some materials, the  $I$ – $V$  curve is not linear, meaning its effective resistance is dependent on both the voltage or current and temperature. For such samples, the temperature–resistance relation has to consider the  $I$ – $V$  effect, which makes the calibration really challenging and thermal probing difficult. Third, since the sample and the copper electrodes (usually used in TET measurement) are on a heating plate during calibration, the stage will thermally expand at the level of  $\mu\text{m}$ . Such small stretching sometimes can break the sample if it is very short and fragile. This will result in calibration failure. Considering the above factors, a new technique is needed to probe the thermal response of sample during thermal excitation without using the resistance as the indicator for temperature probing. This is intended to eliminate all the above problems and provide better thermal conductivity measurement.

Johnson noise, caused by the thermal agitation of the charge carriers (usually electrons), generates an open-circuit voltage across any resistance, which is random with a zero mean over a long time. It always happens regardless of any applied bias. In a realistic resistor, it is almost a white noise, which means the power spectral density is nearly constant throughout the frequency domain up to GHz [10]. Johnson noise is first observed by Johnson. The value of the generated voltage is only dependent on temperature and resistance. Voltage variance (mean square) per hertz of bandwidth is given by the Nyquist relation [11]:  $\overline{V_n^2} = 4k_B TR$ . Here  $R$  is resistance in ohms,  $T$  is the temperature in Kelvin for the resistor, and  $k_B$  is the Boltzmann constant ( $1.381 \times 10^{-23}$  J/K). Johnson noise thermometer (JNT) has been developed according to this principle. Johnson noise thermometers developed by Kinsner et al. [12] are claimed to be useful in harsh environments such as the nuclear power plant. In their work, the temperature measurement resistor is connected in parallel to two separate preamplifiers. The power spectral density from the first one is correlated with that from the other to form power spectral density (CPSD) in order to eliminate the preamplifier electronic noise. It is not necessary to take the preamplifier noise into consideration even though it varies. Another way to obtain Johnson noise was also introduced to avoid the use of resistance value in determining temperature. In this technique, the temperature measurement resistor is connected in series with an inductor and a capacitor. This design forms a tuned circuit so that no sensor resistance is needed in the output and a relative smaller frequency range can be used to do the test [13]. The Johnson noise thermometry developed by National Institute of Standards and Technology (NIST) and Measurements Standards Laboratory is calibrated with a quantum-accurate pseudo-noise voltage wave form. During their Johnson noise measurement, cross-correlation Johnson noise is obtained, and then the noise power spectral density is integrated over a wide bandwidth and the upper frequency is as high as 1 MHz [14–17]. Borkowski et al. [18] developed a new method of Johnson noise thermometry to measure high temperatures. It is claimed to measure temperature as high as 1300 K. Fong et al. developed a measurement system based on high-frequency Johnson noise to probe the wide bandwidth interface thermal conductance at temperatures as low as several Kelvins. The sensitivity of their noise thermometry  $\delta T_e$  follows the Dicke radiometer formula:  $\delta T_e / (T_e + T_s) = (B t_m)^{-1/2}$ , where  $t_m$  is the measurement time,  $T_s$  is the noise temperature of the system, and  $B$  is the measurement bandwidth. With a bandwidth of 80 MHz, the sensitivity is claimed to be as low as  $2 \text{ mK}/\sqrt{\text{Hz}}$ . In their work, Johnson noise is first rectified by a diode, and then, the noise power spectral density is obtained [19, 20]. So

far, even though the Johnson noise thermometer can be very sensitive and accurate when measuring temperatures from below 1 mK to over 1000 K, there is no practical Johnson noise thermometer for general use [21].

From the Dicke radiometer formula, we can know that a faster readout is obtained with hundreds MHz bandwidth. But this needs to do impedance matching to maximize the transmission of Johnson noise from the sample to the amplifier due to the effect of sample-to-preamplifier cable capacitance. Hundreds of kHz bandwidth will lead to a slower readout, but it is not necessary to do the impedance matching for this bandwidth. In most of the former work about Johnson noise thermometer, the measurement works in ultra-high-frequency range. It is necessary to do impedance matching to maximize the transmission of Johnson noise from the resistance to the preamplifier. The reflection/transmission due to impedance mismatch of the whole circuit has to be calibrated carefully before temperature measurement. If not handed well, the Johnson noise during high-frequency domain will be partly blocked due to the effect of resistance-to-preamplifier cable capacitance. There were some reported Johnson noise thermometers operated at low frequencies. Brixy used a Johnson noise thermometer with a Johnson noise frequency range of 10–50 kHz with the combination of resistor and capacitor to detect the temperature in a reactor. Good consistency between the temperature obtained from Johnson noise thermometer and thermal couple was obtained [22]. A switching type thermometer developed by Pickup was used to measure Johnson noise between 10 and 100 kHz and average over 10 h. The resulting temperature measurement could have a high resolution (3 mK at 100 K) [23]. By comparing the Johnson noise within the frequency range of 10–100 kHz for two resistors (one under known temperature and the other one for unknown temperature measurement), the uncertainty for temperature measurement was achieved lower than  $\pm 0.1$  K [24]. In this paper, what we try to do is not to measure temperature but to characterize thermal conductivity of microfiber by using Johnson noise. A measurement system is developed to obtain the thermal conductivity of microfibers by making use of measuring Johnson noise within the low-frequency range under different temperatures. It is not necessary to do the impedance matching and calibration of the transmission. Also this kind of low-frequency range is favorable for the sample which is coated with a metallic film that could not sustain high-frequency noises. When it comes to the noise of the preamplifier electronics, it has been proven to be constant with a variation less than 1 % in the experiment. So in this paper, the Johnson noise is directly measured by a dynamic signal analyzer but not the CPSD.

The paper is organized as follows. First, we evaluate the Johnson noise measurement accuracy by measuring the

Boltzmann constant. This is also intended to evaluate the signal transmission efficiency of the whole circuit. Second, the temperature of a resistor under different laser heating powers is obtained through two ways: One is from Johnson noise measurement, and the other one is from the relationship between the temperature and resistance of the resistor. This is to directly evaluate the temperature measurement accuracy. Finally, the thermal conductivity of a glass fiber is characterized by measuring the Johnson noise of the sample. The thermal characterization accuracy is evaluated by comparing with the measurement result using the TET technique.

## 2 System response and thermal measurement accuracy

### 2.1 System response of preamplification

Johnson noise is very small. For instance, given the resistance is 1 k $\Omega$  and Johnson noise is measured under room temperature, the order of the Johnson noise is  $\sim 10^{-17}$  V<sup>2</sup>/Hz. It is necessary to amplify it before using a dynamic signal analyzer to detect it. So before we conduct thermal transport study using Johnson noise, the system response and measurement accuracy are fully evaluated. In this experiment setup, the to-be-measured resistor is placed in a chamber in order to minimize external noise injection. The Johnson noise across the resistor is first amplified by a low noise amplifier (SR560). The amplifier output is connected to a dynamic signal analyzer (SR785) through a coaxial cable. All the coaxial cables in this experiment are wrapped with aluminum foil to eliminate the effect of external noise. In this experiment, carbon film resistors with different resistance values are used under room temperature to measure their Johnson noise. The voltage spectral density from 50 to 102.4 kHz is used for noise evaluation. Thousand root mean square (RMS) data averages are collected to minimize statistical fluctuations. Instrument noise resulted from the amplifier and dynamic signal analyzer has been proven to be constant with a variation less than 1 % during the experiment.

The voltage spectral density of Johnson noise is shown in the inset of Fig. 1 for several resistors with different resistance. We could see that the spectrum is flat. This is consistent with the fact that Johnson noise is constant over a very wide frequency range. The average voltage spectral density of Johnson noise (averaged over 50–102.4 kHz of the spectrum) is shown in Fig. 1 for resistance ranging from 99 to 4630  $\Omega$ . The voltage spectral density can be expressed as  $S_V = G^2(4k_B T R + S_0)$ , where  $S_0$  is the output voltage noise of the preamplifier,  $G$  is the gain of the preamplifier, and  $T$  is the room temperature. In our experiment, the gain is 80 dB. It is constant among the

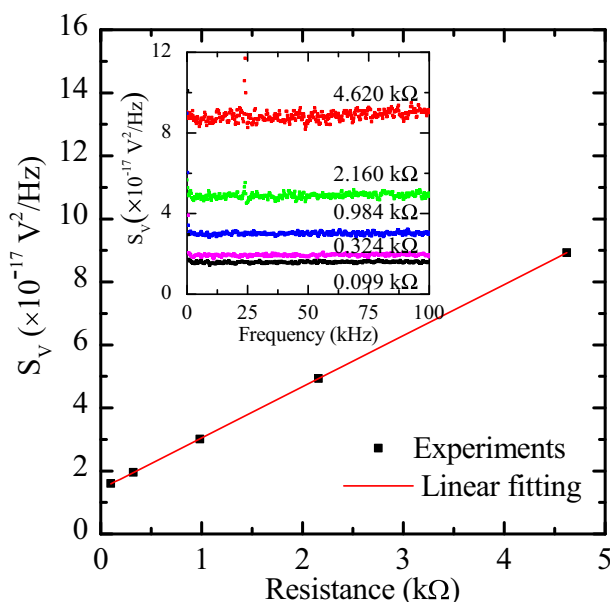


**Fig. 1** Variation of measured Johnson noise voltage spectral density against resistance. For each resistance, the voltage spectral density from 50 to 102.4 kHz is averaged and used. Excellent linear relation is observed between them. The fitting is used to determine the Boltzmann constant. Based on the fitting,  $k_B$  is determined as  $1.375 \times 10^{-23}$  J/K, agreeing well with the standard Boltzmann constant ( $1.381 \times 10^{-23}$  J/K). From the fitting, we also determine the input noise of the preamplifier which is  $1.424 \times 10^{-17}$  V<sup>2</sup>/Hz. The *inset* figure shows the voltage spectral density of Johnson noise measured across different resistors, and clear Johnson noise increase is observed for an increased resistance

frequency domain. Figure 1 shows a very good linear relationship between the measured voltage spectral density of Johnson noise with the resistance of different resistors. When the resistance goes down to zero, the measured noise is supposed to be the output noise of the preamplifier. Linear fitting based on the above equation is conducted. In the manual of SR560, when frequency is between 1 and 100 kHz, and the source resistance is between 10  $\Omega$  and 10 k $\Omega$ , the preamplifier's own noise remains constant. In this fitting,  $S_0$  could be assumed constant considering the frequency range and resistances of the resistors used in this experiment and it is determined as  $1.424 \times 10^{-17}$  V<sup>2</sup>/Hz. This value is very reasonable since the output noise of SR560 is given 4 nV/ $\sqrt{\text{Hz}}$  in the data manual, namely  $1.6 \times 10^{-17}$  V<sup>2</sup>/Hz. The slope of the fitting is  $4k_B T$  according to the Nyquist relation. In this experiment, the slope is determined as  $1.62 \times 10^{-20}$  J. The Boltzmann constant is obtained by dividing the slope with  $4T$ . We read the room temperature from a thermometer in our laboratory. The room temperature is 295.1 K when the experiment is conducted. The specific value of the Boltzmann constant is determined to be  $1.375 \times 10^{-23}$  J/K. This result agrees nicely with the standard value of Boltzmann

constant ( $1.381 \times 10^{-23}$  J/K) with a relative error of 0.36 %. So we feel very confident of the preamplifier, dynamic signal analyzer and the connections in the experiment.

## 2.2 Temperature measurement accuracy evaluation

In the above section, the measurement accuracy which includes amplification and signal transmission of the whole system is carefully studied and verified. Then we design an experiment to test the temperature measurement accuracy before we apply the technique for temperature probing for thermophysical properties measurement. The inset in Fig. 2a shows the schematic setup of this accuracy test. Here, a resistance temperature detector (RTD) is used as the sample in this experiment. It is placed in a vacuum chamber to minimize the environment influence such as air flow and fluctuation. A laser beam is used to heat the RTD. Different from using a voltage source to heat the sample, the laser will not cause any voltage noise in the sample. As the laser energy level is increased, the temperature of the RTD will increase as well and thus causes its resistance to rise. The resistance of RTD has an exact relationship with temperature  $R_t = R_0(1 + At + Bt^2)$ , where  $R_0$  is the resistance at 0  $^\circ\text{C}$ ,  $t$  is temperature in degrees celsius, and  $A$  and  $B$  are coefficients given by the product data. The temperature of the RTD can be obtained exactly from the resistance which is measured by using a 6 $\frac{1}{2}$  digital multi-meter (Agilent 34401A). In order to measure the resistance accurately, a 10 k $\Omega$  measurement range is chosen, and the operating current is 100  $\mu\text{A}$ . The temperature of the RTD can also be obtained by measuring the Johnson noise and compared with the one determined by using resistance. This will provide excellent evaluation of the direct temperature measurement accuracy based on Johnson noise.

The voltage spectral density during frequency domain is shown in Fig. 2a. The five peaks in the spectrum are caused by the external noise. Data lying on or close to the baseline is used to calculate the temperature of RTD. The voltage spectral density and temperature has the following relationship  $S_V = G^2(4k_B TR + S_0)$ . The output noise of the preamplifier remains constant during the experiment, so we use  $1.424 \times 10^{-17}$  V<sup>2</sup>/Hz for  $S_0$  to calculate the temperature. We mainly focus on the amount of temperature increase since our later experiment aims at probing the thermal conductivity, the temperature increase is used to determine the thermal conductivity. The exact temperature of the sample is less important in our experiment. By comparing the temperature rise obtained from calculation of Johnson noise and resistance of RTD, respectively, the accuracy of temperature measurement of JET is determined. Figure 2b shows the result of the temperature



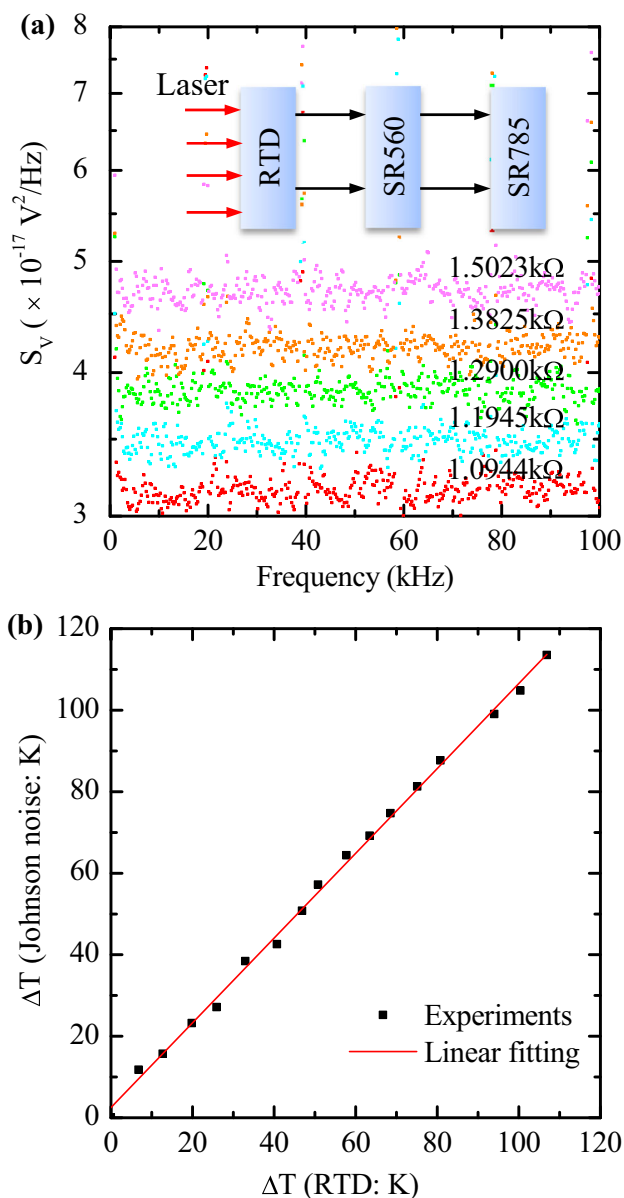


**Fig. 2** **a** Voltage spectral density of Johnson noise measured across the RTD. The *inset* shows the schematic setup for evaluation of temperature measurement accuracy. *RTD* resistance temperature detector, *SR560* preamplifier, *SR785* dynamic signal analyzer. **b** Temperature rise obtained through Johnson noise and RTD, respectively. The slope of the fitting line is 1.04. It means that temperature increase obtained from the Johnson noise method is very reasonable and reliable, having a very small deviation of 4 % from the RTD method

measurement accuracy evaluation. The temperature rise is obtained by subtracting the temperature with zero laser heat input power. The slope of the fitting line is 1.04. It means that temperature increase obtained from the Johnson noise method is very reasonable and reliable. Compare with the standard method using RTD, it has a very small deviation of 4 %.

### 3 Physics and experimental details for Johnson noise electro-thermal characterization

#### 3.1 Experimental principle and setup

Schematic of the setup to measure the thermal conductivity of a one-dimensional material based on Johnson noise is shown in Fig. 3a. In this Johnson noise electro-thermal (JET) technique, if the sample is non-conductive, it will be first coated with iridium in order to make it conductive. Then the sample is suspended between two copper electrodes. The sample is connected with a resistor which has a greater value of resistance (we use  $R_0 = 55.93 \text{ k}\Omega$  in this experiment). A voltage source (*SIM928*) is used in this electrical circuit to offer a current to induce Joule heating in the sample. Both sample ( $R_s$ ) and the resistor ( $R_0$ ) are placed in a vacuum chamber in order to eliminate effect of external noise. The two terminals of the sample are also connected to the feedthrough of the chamber. And then

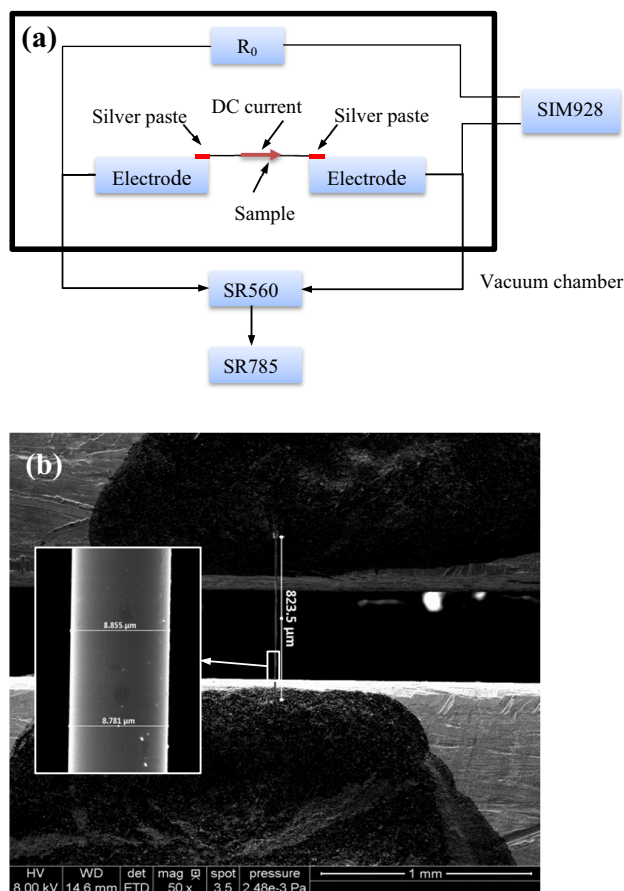


**Fig. 3** **a** Schematic of the setup for the JET technique, *SR560* preamplifier, *SR785* dynamic signal analyzer, *SIM928* voltage source,  $R_0$  resistor which has a large resistance. **b** SEM images of the glass fiber measured in this work. The *inset* shows details of the diameter and surface morphology

another terminal of the feedthrough is connected to the preamplifier (SR560) through a coaxial cable. The output of the preamplifier is connected to the dynamic signal analyzer (SR785) through a coaxial cable. All the coaxial cables are wrapped with aluminum foil to minimize the effect of external noise.

Some points need to be explained here. First, the sample is very fine and fragile, so a resistor ( $R_0$ ) with a large resistance is used to limit the current in the sample and thus protect it. Second, we measure the bias over the sample ( $V_{R_s}$ ) by using a digital multi-meter (Agilent 34401A), assuming that the resistance of  $R_0$  remains constant during the whole experiment. This is reasonable since the heating power for this resistor is very negligible. Therefore, the real resistance of the sample is obtained through calculation as  $R_0 V_{R_s} / (V - V_{R_s})$  where  $V$  is the overall voltage applied to the circuit. Third, what we obtained is only the Johnson noise without shot noise. When the length of sample is much larger than the electron–photon scattering length ( $L \gg l_{e-ph}$ ), the shot noise vanishes [25, 26]. The electron's thermal conductivity can be expressed as  $k = C v_F l_{e-ph} / 3$  [27] for the thermal conductivity of particles of velocity  $v_F$ , heat capacity  $C$  per unit volume and mean free path  $l_{e-ph}$ . The electron mean free path  $l_{e-ph}$  of iridium is calculated to be 2.04 nm [28]. The length of the sample used in the experiment is much larger than 2.04 nm. Fourth, the voltage source also has input voltage noise even though it is much smaller than that of a current source. Its effect on  $R_s$  and  $R_0$  can be calculated like voltage of two resistors in series. The measured voltage spectral density is expressed as:

$$S_V = \left( \frac{R_0}{R_0 + R_s} \right)^2 \cdot 4k_B T_s R_s + \left( \frac{R_s}{R_0 + R_s} \right)^2 \cdot (4k_B T_0 R_0 + \langle V_0^2 \rangle) + S_0 \quad (1)$$

where  $T_0$  is room temperature and also the temperature of  $R_0$ ,  $T_s$  is the sample temperature,  $\langle V_0^2 \rangle$  is the output noise of the voltage source, and  $S_0$  is the output noise of the preamplifier. Since  $R_0$  is much larger than  $R_s$  (approximate 83 times in this experiment), the measured voltage spectral density can be approximately equal to  $4k_B T_s R_s + S_0$  with a very high accuracy. The relative error of this approximation is smaller than 2 % in this experiment. If the sample is directly connected with the voltage source, the measured voltage spectral density is:

$$S_V = 4k_B T_s R_s + \langle V_0^2 \rangle + S_0 \quad (2)$$

Thus, the value of output noise of voltage source is larger than that of the Johnson noise of the sample and the effect of voltage source becomes not negligible. A resistor with a much larger resistance is helping to minimize the

effect of output noise of voltage source on the Johnson noise measurement.

### 3.2 Physics model development

Figure 3a shows that under DC current heating, the heat transfer in the sample is a one-dimensional heat conduction problem. Santavicca et al. developed a 1D energy loss model for electrons in single-walled carbon nanotubes. In their work, the hot electron diffusion, the energy dissipation to the tube and phonon emission were taken into consideration ( $p_{ph}$ ). Different from us, they measured  $p_{ph}$  in experiment. But in our analysis, we derive the final average temperature rise under the effect of radiation [29]. In this experiment, the electrical heating power has the form of  $I^2 R_s$ . It varies with the change of the resistance of the sample. Since the copper electrodes used in this experiment are much larger than the sample dimension, the temperature of the electrodes can be assumed constant even though a small current is flowing through them. The boundary conditions can be described as  $\Delta T(x=0) = 0$ , where  $\Delta T = T - T_0$ ,  $T_0$  is the room temperature. The governing equation is

$$\frac{\partial(\rho c_p T)}{\partial t} = k \frac{\partial^2 T}{\partial x^2} + \dot{q} - \frac{16\epsilon\sigma(T - T_0)T_0^3}{D}, \quad (3)$$

where  $\rho$ ,  $c_p$  and  $k$  are the density, specific heat and thermal conductivity of the sample, respectively,  $\dot{q}$  is electrical heating power per unit volume. It has the form of

$$\dot{q} = \frac{I^2 R_s}{AL}, \quad (4)$$

where  $R_s$  is the resistance of the sample and it can be detected instantly when measuring the Johnson noise, and  $A$  and  $L$  are the cross sectional area and length of the sample, respectively.  $16\epsilon\sigma(T - T_0)T_0^3/D$  describes the effect of radiation for small temperature increases [ $(T - T_0)/T_0 \ll 1$ ],  $\epsilon$  and  $\sigma$  the emissivity and Stefan–Boltzmann constant, and  $D$  is the sample diameter. When it reaches steady state,  $\partial(\rho c_p T)/\partial t = 0$ , and the final average temperature rise which is averaged over the sample length is:

$$\Delta T = \frac{I^2 R_s}{LAa} \left( 1 - \frac{\tanh(mL/2)}{(mL/2)} \right), \quad (5)$$

where  $a$  is  $16\epsilon\sigma T_0^3/D$  and  $m$  is  $\sqrt{a/k}$ . Völklein et al. [30] got similar temperature derivation for 1D heat transport in single metallic nanowires. They also neglected the effect of heat convection and take the radiation and conductive thermal transport into consideration. Normally, the thermal conductivity of a glass fiber is  $\sim 1.2$ – $1.4$  W/m K at room temperature. The effective thermal conductivity due to the radiation effect is determined according to the equation  $16\epsilon\sigma T^3 L^2 / (D\pi^2)$  [31]. It is around 0.1 W/m K for the

glass fiber used in this experiment using an emissivity of 0.5. The exact effect of radiation will be subtracted to get the real thermal conductivity of glass fiber. Details about this consideration are given in a later section.

### 3.3 Methods for data analysis to determine thermal conductivity of the sample

From the above description, the sample and resistor are in series, and a voltage source is used to offer a current to induce Joule heating. The overall voltage ranges from 5 to 20 V with a step of 0.5 V. We use the voltage over the sample, the voltage over the sample and resistor and the resistance of resistor  $R_0$  to obtain the resistance of the sample and thus obtain the current in the sample. After obtaining the voltage spectral density of Johnson noise, the data in the frequency range of 50–102.4 kHz are used to calculate the RMS data average. Thousand root mean square (RMS) data averages are collected to minimize the statistical fluctuations. The total voltage spectral density is

$$S_V = G^2[4k_B(T_0 + \Delta T)R_s + S_0] \quad (6)$$

where  $S_0$  is the output noise of preamplifier,  $\Delta T$  is  $I^2R_s/LAa \cdot [1 - \tanh(mL/2)/(mL/2)]$ , and  $G$  is the gain of the preamplifier. Here,  $S_0$  is  $1.424 \times 10^{-17} \text{ V}^2/\text{Hz}$  which is determined in the above experiment when determining the Boltzmann constant. Then the temperature rise is calculated out according to Eq. (6). After obtaining the temperature rise, we plot the temperature rise ( $\Delta T$ ) against the input power of the sample ( $I^2R_s$ ) and fit it with Eq. (5) to obtain thermal conductivity.

### 3.4 Results and discussion

The SEM images of the glass fiber measured in this work are shown in Fig. 3b. The inset shows details of the diameter and surface morphology. The diameter and length of the sample are 8.82 and 823.5  $\mu\text{m}$ . The initial sample resistance is 673  $\Omega$ . During the JET test, the sample is placed in a vacuum chamber. The pressure of the chamber is remained under 2 mTorr to minimize the convection heat transfer effect. A DC voltage bias ranging from 5 to 20 V is applied to this electrical circuit. Figure 4a shows the voltage spectral density of Johnson noise measured under two different overall voltages. Figure 4b shows the sample resistance variation against the input power of the sample; sound linear fitting is obtained between sample resistance and the input power of the sample. This is physically expectable since the temperature rise is linearly proportional to the heating level within a moderate heating range, and the electrical resistance changes with temperature linearly. We fit the temperature rise against input power of the sample according to Eq. (5), and the experiment data and

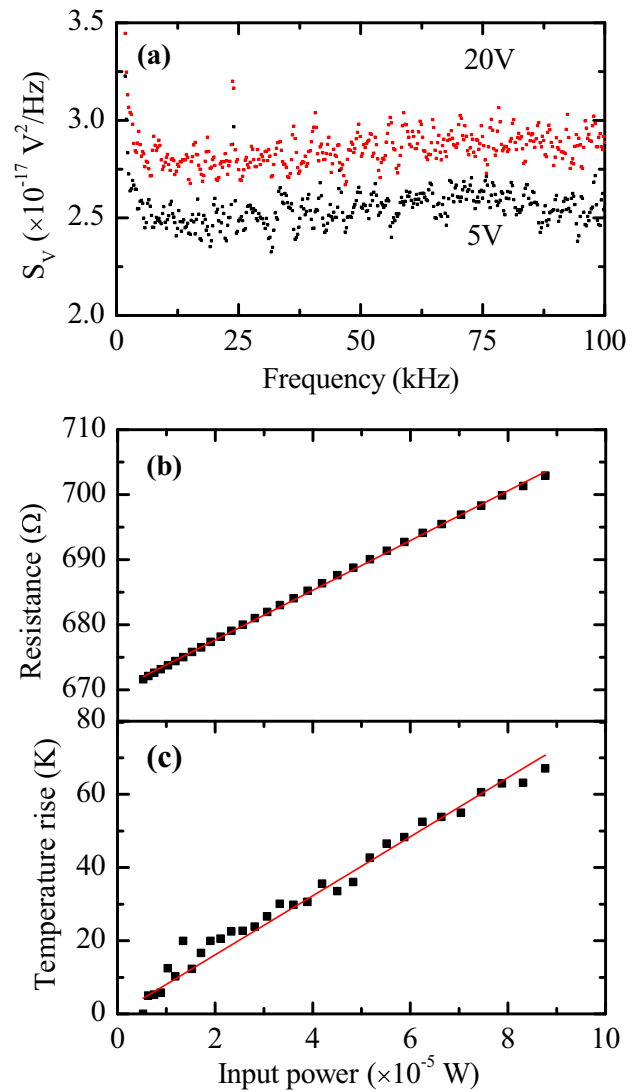


**Fig. 4** **a** Voltage spectral density of Johnson noise measured with two applied bias. **b** The fitting of sample resistances against input power of the sample. **c** Variation of temperature rise against input power of the sample. The thermal conductivity of the fiber is determined by fitting the  $\Delta T \sim I^2R_s$  relation using Eq. (5). The sample's thermal conductivity is determined as 1.31 W/m K (inclusive of the iridium effect). Details are provided in the paper to subtract the iridium effect

fitting data are shown in Fig. 4c. The glass fiber and iridium have emissivities of 0.92 and almost 0 at room temperature. In this experiment, we use an emissivity of 0.5 in the fitting (upper part of the glass fiber is coated with iridium and the lower half is not). The instrument input noise takes  $1.424 \times 10^{-17} \text{ V}^2/\text{Hz}$ , and the sample's thermal conductivity with the effect of iridium is characterized as 1.31 W/m K. Equation (5) has taken the effect of radiation into consideration but not the effect of iridium. The real thermal conductivity of glass fiber is obtained according to Eq. (7) as

$$k = k_{e0} - \pi\delta/4D \cdot k_{Ir} \quad (7)$$

where  $k_{e0}$  is the measured thermal conductivity obtained in original fitting,  $\delta$  is the thickness of iridium, and  $k_{Ir}$  is the thermal conductivity of iridium. The thermal conductivity of iridium is determined to be 60 W/m K [28]. Thus, the real thermal conductivity of glass fiber is determined as 1.20 W/m K.

We also use the same sample to do TET test to acquire the thermal conductivity. The TET technique has been widely used to measure the thermal diffusivity/conductivity with very high accuracy. During the TET test, the sample is placed in a vacuum chamber and the pressure of the chamber is remained under 2 mTorr. DC current is feed through the sample to induce Joule heating. The temperature rise of the sample causes the resistance of sample to rise, and thus, the voltage over the sample increases. We use an oscilloscope to monitor the voltage evolution and then save the data. We know that the heat transfer problem is one-dimensional along the fiber, the normalized temperature rise, which is defined as  $T^*(t) = [T(t) - T_0]/[T(t \rightarrow \infty) - T_0]$ , can be written as [9]

$$T^* = \frac{96}{\pi^4} \sum_{m=1}^{\infty} \frac{1 - \exp[-(2m-1)^2 \pi^2 \alpha t / L^2]}{(2m-1)^4} \quad (8)$$

where  $T(t)$  is the average temperature of the sample along the fiber,  $T_0$  is the room temperature,  $\alpha$  is the real thermal diffusivity,  $L$  is the length, and  $t$  is the time. After obtaining the temperature evolution  $T-t$ , we use least square fitting to obtain the thermal diffusivity of the sample. The normalized temperature rise is calculated according to Eq. (8) by using different trial values in a MATLAB program. The trial value giving the best fit of the experimental data is regarded as the measured thermal diffusivity of the sample. The thermal conductivity ( $k_{e0}$ ) of the glass fiber without the effect of radiation can be calculated as

$$k_{e0} = \alpha_e \rho c_p - \frac{16\epsilon\sigma T^3 L^2}{\pi^2 D} \quad (9)$$

where  $\alpha_e$  is the measured thermal diffusivity and  $T$  is the average temperature of the sample during TET test. In this TET test, the current is ranging from 0.16 mA to 0.24 mA with a step of 0.02 mA. Figure 5 shows a typical experiment data and the fitting line. The measured thermal diffusivity ( $\alpha_e$ ) is determined as  $9.40 \times 10^{-7} \text{ m}^2/\text{s}$ . The density and heat capacity of the glass fiber are determined to be 2070 kg/m<sup>3</sup> [28] and 745 J/kg K [32] at room temperature. The thermal conductivity of glass fiber after subtracting the effect of radiation is calculated as 1.34 W/m K according to Eq. (9). According to Eq. (7), the real thermal conductivity of glass fiber is determined to be 1.26 W/m K after ruling out the effect of iridium. This value agrees very well with that obtained using the JET

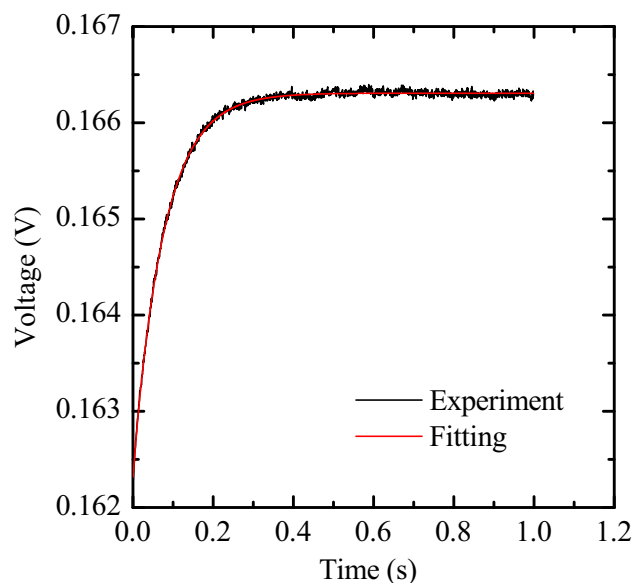


**Fig. 5** TET fitting result curve when a square current of 0.24 mA is applied to the sample. The measured thermal diffusivity ( $\alpha_e$ ) is determined as  $9.40 \times 10^{-7} \text{ m}^2/\text{s}$  (inclusive of the radiation and iridium effects). Details are provided in the paper to subtract the radiation and iridium effect

technique 1.20 W/m K. This strongly proves the high measurement accuracy of the JET technique we are reporting in this work. The thermal conductivities obtained through these two methods are consistent with the reference value which is 1.3 W/m K.

Here, we discuss the measurement uncertainty of the JET technique. According to the temperature measurement accuracy evaluation test, the temperature measurement uncertainty is 4 %. During the temperature rise–input power of the sample fitting, the fitting uncertainty is 1.5 %. The diameter and length of the glass fiber are measured by using a scanning electron microscope. The relative errors of the diameter and length are both less than 1 %. The final measurement uncertainty of thermal conductivity is estimated less than 5 %.

## 4 Conclusions

In this paper, a novel technique was developed to directly characterize the thermal conductivity of one-dimensional microscale materials based on Johnson noise measurement. The circuit and setup efficiency in terms of signal transmission was fully evaluated by measuring the Boltzmann constant through Johnson noise. The Boltzmann constant was found to be  $1.375 \times 10^{-23} \text{ J/K}$ , and it is consistent with the reference value of  $1.381 \times 10^{-23} \text{ J/K}$ . The temperature measurement accuracy was also fully studied, and good measurement accuracy was obtained (better than



4 %). The JET technique was employed to measure the thermal conductivity of a glass fiber of 8.82  $\mu\text{m}$  diameter. The thermal conductivity of the glass fiber was found to be 1.20 W/m K and agrees very well with the value of TET measurement and the reference value. Our uncertainty analysis showed that the JET technique has an uncertainty less than 5 %. The JET technique was proved to be a quick and reliable way to characterize the thermal conductivity of microscale materials. It does not require calibration and impedance matching in terms of Johnson noise measurement since low-frequency Johnson noise was used in our technique. In many other techniques for thermal conductivity measurement, a resistance ( $R$ )–temperature ( $T$ ) relation has to be used for temperature measurement. Calibration is usually needed to establish the  $R$ – $T$  relation. Since some materials' electrical resistance can be changed permanently during the test, if the resistance and the temperature are obtained at different times, the accuracy of the experiment is sacrificed. In the JET technique, the resistance and Johnson noise of the sample are obtained simultaneously; therefore, the accuracy of the experiment can be significantly improved. Besides, since the TET technique could measure the thermal diffusivity successfully and the JET technique could measure the thermal conductivity directly, these two techniques can be combined to determine the volumetric specific heat of a material with high accuracy.

**Acknowledgments** Support of this work by the Army Research Office (W911NF-12-1-0272), Office of Naval Research (N000141210603) and National Science Foundation (CBET1235852, CMMI1264399) is gratefully acknowledged. We are grateful to MO-SCI Corporation for providing the glass fiber samples used in this work. X.W thanks the partial support of the “Taishan Scholar” Program of Shandong, China.

## References

1. W. Yi, L. Lu, D.L. Zhang, Z.W. Pan, S.S. Xie, *Phys. Rev. B* **59**, R9015 (1999)
2. T. Choi, D. Poulikakos, J. Tharian, U. Sennhauser, *Nano Lett.* **6**, 1589 (2006)
3. P. Kim, L. Shi, A. Majumdar, P.L. McEuen, *Phys. Rev. Lett.* **87**, 215502 (2001)
4. P. Kim, L. Shi, A. Majumdar, P.L. McEuen, *Physica B* **323**, 67 (2002)
5. L. Shi, D. Li, C. Yu, W. Jang, D. Kim, Z. Yao, P. Kim, A. Majumdar, *J. Heat Transf.* **125**, 881 (2003)
6. J. Hou, X. Wang, L. Zhang, *Appl. Phys. Lett.* **89**, 152504 (2006)
7. J. Guo, X. Wang, D.B. Geohegan, G. Eres, C. Vincent, *J. Appl. Phys.* **103**, 113505 (2008)
8. X. Feng, X. Wang, X. Chen, Y. Yue, *Acta Mater.* **59**, 1934 (2011)
9. J. Guo, X. Wang, T. Wang, *J. Appl. Phys.* **101**, 063537 (2007)
10. J.B. Johnson, *Phys. Rev.* **32**, 97 (1928)
11. H. Nyquist, *Phys. Rev.* **32**, 110 (1928)
12. R. Kisner, C. L. Britton, U. Jagadish, J. B. Wilgen, M. Roberts, T. V. Blalock, D. Holcomb, M. Bobrek, M. N. Ericson, *Aerosp. Conf. Proc.* 2586 (2004)
13. M.G. Pepper, J.B. Brown, *J. Phys. E: Sci. Instrum.* **12**, 31 (1979)
14. S.P. Benz, J.M. Martinis, P.D. Dresselhaus, S.W. Nam, *IEEE Trans. Inst. Meas.* **52**, 545 (2003)
15. S.W. Nam, S.P. Benz, P.D. Dresselhaus, C.J. Burroughs, W.L. Tew, D.R. White, J.M. Martinis, *IEEE Trans. Inst. Meas.* **54**, 653 (2005)
16. S.P. Benz, J.F. Qu, H. Rogalla, D.R. White, P.D. Dresselhaus, W.L. Tew, S.W. Nam, *IEEE Trans. Inst. Meas.* **58**, 884 (2009)
17. S. P. Benz, J. M. Martinis, S. W. Nam, W. L. Tew, D. R. White, in *Proceedings Tempmeko 2001: 8th International Symposium on Temperature and Thermal Measurement in Industry and Science, Vol 1 & 2*, 37 (2002)
18. C.J. Borkowski, T.V. Blalock, *Rev. Sci. Instrum.* **45**, 151 (1974)
19. K.C. Fong, K.C. Schwab, *Phys. Rev. X* **2**, 031006 (2012)
20. R.H. Dicke, *Rev. Sci. Instrum.* **17**, 268 (1946)
21. L. Spietz, K.W. Lehnert, I. Siddiqi, R.J. Schoelkopf, *Science* **300**, 1929 (2003)
22. H. Brix, *Nucl. Instrum. Methods* **97**, 75 (1971)
23. C.P. Pickup, *Metrologia* **11**, 151 (1975)
24. L. Crovini, A. Actis, R. Galleano, *IEEE Trans. Inst. Meas.* **42**, 391 (1993)
25. V.A. Khlus, *Sov. Phys. JETP* **66**, 2179 (1987)
26. M. Reznikov, M. Heiblum, H. Shtrikman, D. Mahalu, *Phys. Rev. Lett.* **75**, 3340 (1995)
27. C. Kittel, *Introduction to Solid State Physics*, 5th edn. (Wiley, New York, 1976)
28. H. Lin, S. Xu, X.W. Wang, N. Mei, *Small* **9**, 2585 (2013)
29. D.F. Santavica, J.D. Chudow, D.E. Prober, M.S. Purewal, P. Kim, *Nano Lett.* **10**, 4538 (2010)
30. F. Völklein, H. Reith, T.W. Cornelius, M. Rauber, R. Neumann, *Nanotechnology* **20**, 325706 (2009)
31. G.Q. Liu, S. Xu, T.T. Cao, H. Lin, Y.Q. Zhang, X.W. Wang, *Biopolymers* **101**, 2019 (2014)
32. D.R. Lide, *CRC Handbook of Chemistry and Physics, Internet Version 2015*, 95th edn. (Boca Raton, 2014)